JOURNAL OF GEOPHYSICAL RESEARCH, VOL. 111, F02023, doi:10.1029/2005JF000349, 2006

Erosion rates during rapid deglaciation in Icy Bay, Alaska

Michèle Koppes[1] and Bernard Hallet[1]

Received 6 June 2005; revised 9 March 2006; accepted 17 March 2006; published 24 June 2006.

[1] Contemporary glacial erosion rates based on sediment yields in southeast Alaska merit considerable attention because they are unsurpassed worldwide, and they significantly exceed long-term exhumation rates in the region. Two issues are likely to contribute to these high rates: contemporary sediment yields in fjords (1) have generally been overestimated by failing to account for the considerable input of subaerially derived material and (2) are exceptionally high because tidewater glaciers in southeast Alaska have been anomalously dynamic and erosive during the past century of rapid retreat. To investigate these influences and to quantify the rate at which Tyndall Glacier erodes its basin we present seismic data defining the volume of sediments in Taan Fjord, Icy Bay. We subtract the contribution of subaerially derived sediments from the fjord sediment package to determine the sediment yield directly from Tyndall Glacier during the most recent period of retreat: 1962–1999. Using a numerical model of proglacial glacimarine sedimentation, we then calculate the annual sediment yield from, and the corresponding erosion rate of, Tyndall Glacier during this period, which averages 28 ± 5 mma^{-1}. A strong correlation emerges between glacial retreat rates and glacial sediment yields, implying that most contemporary sediment yield data from retreating tidewater glaciers may correspond to contemporary erosion rates that are a factor of 3.5 ± 1.5 higher than in the long term. Hence we estimate the long-term erosion rate for Tyndall Glacier to be 9 ± 2 mma^{-1}.

Citation: Koppes, M., and B. Hallet (2006), Erosion rates during rapid deglaciation in Icy Bay, Alaska, *J. Geophys. Res.*, *111*, F02023, doi:10.1029/2005JF000349.

1. Introduction

[2] Glacial erosion has become a principal issue in contemporary research on landscape evolution, as it plays an integral role in the coupling of tectonics and climate in most major mountain ranges through its influence on exhumation and the evacuation of crustal material from orogens. The climate-sensitive rate and spatial distribution of erosion can be as important as the tectonic environment in controlling the size, morphology and structural development of mountain ranges [e.g., *Molnar and England*, 1990; *Raymo and Ruddiman*, 1992; *Brozovic et al.*, 1997; *Beaumont et al.*, 2000; *Montgomery et al.*, 2001; *Tomkin*, 2003]. Moreover, rapid rock uplift may be localized in regions of rapid erosion due to important feedbacks emerging between topography, exhumation and the vertical advection of material from depth [e.g., *Zeitler et al.*, 2001; *Finlayson et al.*, 2002]. The ''snow buzzsaw'' hypothesis, in which relatively rapid erosion in glacial and periglacial environments effectively limits the elevation of mountain ranges [*Brozovic et al.*, 1997; *Montgomery et al.*, 2001; *Tomkin*, 2003], is intriguing but it lacks solid supporting data. Concerns have arisen regarding much of the evidence suggesting that glacial and periglacial erosion is generally more rapid than fluvial erosion under similar precipitation regimes and geologic settings. To understand the evolution of mountain systems, many of which are currently glaciated and were considerably more extensively glaciated throughout much of the last ~2 million years, we need to define more precisely the role of glaciers in the crustal budget of active mountain systems.

[3] A number of studies have successfully determined sediment yields from tidewater glaciers, taking advantage of the tendency of most of the sediments produced by these glaciers to be trapped in proglacial fjord basins. Most nontidewater glaciers lack these natural sediment traps, making it difficult to measure their sediment yields. Contemporary sediment accumulation near glacier termini in Alaskan fjords has been examined using sequential bathymetric maps, seismic reflection surveys, sediment traps and radioisotope analyses [e.g., *Molnia*, 1979; *Powell*, 1991; *Hunter et al.*, 1996; *Elverhøi et al.*, 1998; *Jaeger and Nittrouer*, 1999; *Koppes and Hallet*, 2002]. Basin-averaged erosion rates are then generally determined by dividing the volume of sediment delivered to the fjords per unit time by the contributing basin area and accounting for the density difference between sediment and bedrock. This assumes that no significant changes in the amount of sediment stored in the upper basin have occurred. We believe this assumption is reasonable considering the massive volumes of postglacial sediments typically found in fjords and consid-

[1]Department of Earth and Space Sciences, University of Washington, Seattle, Washington, USA.

0148-0227/06/2005JF000349$09.00

ering that drainage basins in rugged alpine areas typically have relatively little subglacial and supraglacial sediment storage [*Hallet et al.*, 1996]; this assumption will be further justified in the Implications section. Moreover, because the vast majority of glaciers studied have been in retreat over the past century, the sediment released by them is not likely to be confounded by the reworking of glacial sediments previously deposited in the glacier foreland. Hence the sediments are primarily the result of bedrock erosion of the glaciated drainage basin.

[4] Annual basin-wide erosion rates range from less than 1 mm for high Arctic glaciers up to as high as 100 mm for the large Alaskan coastal glaciers, the highest known erosion rates in the world [*Hallet et al.*, 1996; *Gurnell et al.*, 1996]. The rapid erosion rate of the coastal Alaskan glaciers presumably arises from a number of factors: they are among the largest and fastest glaciers worldwide, they drain the highest coastal mountain range in the world (the Wrangell-St. Elias), they cover well over half of their basin areas, they drain an area that experiences heavy precipitation from North Pacific storms ($2-3$ ma^{-1} according to *Wilson and Overland* [1987]), and they overly bedrock that is pervasively fractured because of extensive shearing along the major strike-slip faults that dissect the area [*Plafker et al.*, 1994; *Bruhn et al.*, 2004; *Spotila et al.*, 2004]. Moreover, these high rates may actually be underestimated because significant volumes of sediment bypass the fjords and are deposited on the continental shelf [*Molnia*, 1979; *Jaeger and Nittrouer*, 1999].

[5] The estimates of contemporary rates of glacial erosion in coastal Alaska are intriguing in that they are considerably higher than regional exhumation rates interpreted from both low-temperature thermochronometry and modeling, which range from a few millimeters per year [*Spotila et al.*, 2004] to $\sim$7 mma^{-1} [*Bird*, 1996]. Although thermochronometric interpretation is inherently difficult and nonunique, the difference between regional erosion and exhumation rates suggests that contemporary erosion rates are not sustainable in the long term (i.e., on the timescale of millennia). If contemporary erosion rates were representative of long-term rates, erosion would quickly outpace uplift and rapidly eliminate the exceptionally high ranges and relief that characterize the area. This cannot be the case because a major range, sufficiently high to sustain large tidewater glaciers, has persisted in the region for the past 5.5 million years [*Lagoe et al.*, 1993].

[6] Reported contemporary glacial erosion rates are currently receiving heightened scrutiny as a result of two recent findings. First, sediment yields from tidewater glaciers may have been substantially overestimated because they are based on measured volumes of sediments in fjords that may include considerable material derived not from the glaciers themselves but from the adjacent glacier-free landscape. In recently deglaciated landscapes, rates of erosion of loose sediments in ice-marginal deposits can be exceptionally high because fjord walls are oversteepened and because base levels of tributary streams that were formerly dammed by the glacier have suddenly dropped [*Meigs et al.*, 2002] because of the removal of the ice dam and, to a lesser degree, to isostatic rebound. Second, in a previous study of Muir Glacier in Glacier Bay, Alaska [*Koppes and Hallet*, 2002], we found that contemporary sediment yields from tidewater glaciers in southeast Alaska are likely to be far greater than long-term yields because these glaciers have been anomalously dynamic and, by inference, erosive as they retreated rapidly throughout the last century.

[7] In this study, we parallel *Koppes and Hallet* [2002], and present new data documenting the volume of postglacial sediment in a fjord recently exposed by the retreat of Tyndall Glacier. We refine the means of determining long-term glacial erosion rates by explicitly accounting for both the contribution of sediment to the fjord from nonglacial sources and the effect of rapid glacial retreat on sediment yield. We determine the fraction of sediment produced by Tyndall Glacier by subtracting from the total volume in the fjord the volume of sediment derived from two predominant subaerial sources, a pair of now-perched sediment-filled basins that formerly graded to the glacier surface. We also examine the effect of terminus retreat on sediment yield to arrive at an estimate of glacial erosion rates on timescales much longer than the 40 years of retreat covered in this study, and to offer insight into controls on glacial erosion rates.

2. Taan Fjord

[8] Tyndall Glacier, in Wrangell-St. Elias National Park, south-central Alaska, descends steeply from the southwest flank of Mount St. Elias to sea level in Icy Bay, a dramatic drop of over 5400 m in under 18 km. Taan Fjord was most recently deglaciated starting in 1961 when Tyndall glacier separated and retreated from the main trunk of Guyot Glacier in Icy Bay (see Figure 1). The glacier has since retreated 17.25 km in 30 years from its mouth in Icy Bay. In 1991, the terminus stabilized at a shallow bedrock constriction (Hoof Hill) at the head of the fjord, where it is still located (Figure 2).

[9] Continuous sedimentation from the glacier and from tributary valleys has accompanied retreat, filling the fjord bottom with as much as 90 m of sediment locally, and producing some of the highest short-term sedimentation rates ever reported [*Porter*, 1989]. We imaged the fjord bottom sediments using acoustic radio echo sounding from a 750 Hz bubble pulser in the summer of 1999 (see Figure 2 for track lines). Our profiling revealed three dominant facies in the fjord, all underlain by a strong, acoustically impenetrable reflector: (1) a laminated, semi-transparent layer presumed to be predominantly ice-distal glacimarine input with some subaerial fines; (2) a hummocky, chaotic facies presumed to be ice-proximal; and (3) laminated and hummocky facies along the fjord walls associated with landslides and delta fan complexes prograding into the fjord from tributary streams (Figure 3). The reflector underlying all three facies is interpreted to be the surface of the substrate that was compacted by glacial overriding during the Little Ice Age advance that started around 1400 A.D. [*Porter*, 1989]. These facies are characteristic of other Alaskan fjords [e.g., *Molnia et al.*, 1984]. They are also evident in the seismic data collected by the USGS using a minisparker system on the M/V Growler in lower Taan Fjord in 1981 [*Post*, 1983], which we used to verify the accuracy of our identification and digitization of recently added sediment to the fjord.

Figure 1. Tyndall Glacier and Mount St. Elias, with Icy Bay in the foreground, 1938. Tyndall Glacier is joined with Guyot Glacier in the bottom left of the photograph. Between 1938 and 1961 the terminus retreated approximately 3 km until it separated from Guyot Glacier at the mouth of Taan Fjord. Since 1961, it has retreated a further 17.25 km upfjord to its current terminus position at Hoof Hill (dashed line) (photo kindly provided by B. Washburn).

[10] The majority of the recently deglaciated fjord south of the current terminus has been cut into the Yakataga Formation, a tectonically uplifted, massive glacimarine sedimentary sequence dating as far back as 5.5 Ma [*Lagoe et al.*, 1993]. The sediment currently being deposited in the fjord is therefore similar in texture and composition to the underlying "bedrock." The recent sediment deposited since retreat, however, can be distinguished seismically as transparent facies above a clear reflector. This reflector is interpreted to be the upper surface of either denser Yakataga bedrock or more recent glacimarine sediment that was consolidated by overriding ice and/or overlying sediment evacuated by the glacier during the last advance. The bedrock constriction at the current terminus of Tyndall Glacier marks the east-west trending contact between the Yakataga Formation to the south, and the Poul Creek and Kultieth Formations to the north, metasedimentary crystalline lithologies that underlie the entire current glacier basin and form the Mount St. Elias massif. Hence the sediment yields we report in this study from Tyndall glacier over the last half century are high despite the relatively resistant bedrock lithologies underlying most of the glacier.

3. Sediment Influx Into Taan Fjord

3.1. Reconstructing Postglacial Sediment Volume

[11] To determine the total volume of sediment deposited in Taan Fjord over the past 40 years, we calculated the difference between the 1999 sediment surface and the strong underlying reflector. Much like previous workers [e.g., *Molnia*, 1979; *Molnia et al.*, 1984; *Powell*, 1991; *Hunter et al.*, 1996], we assumed that no part of the transparent and chaotic seismic facies represent glacigenic

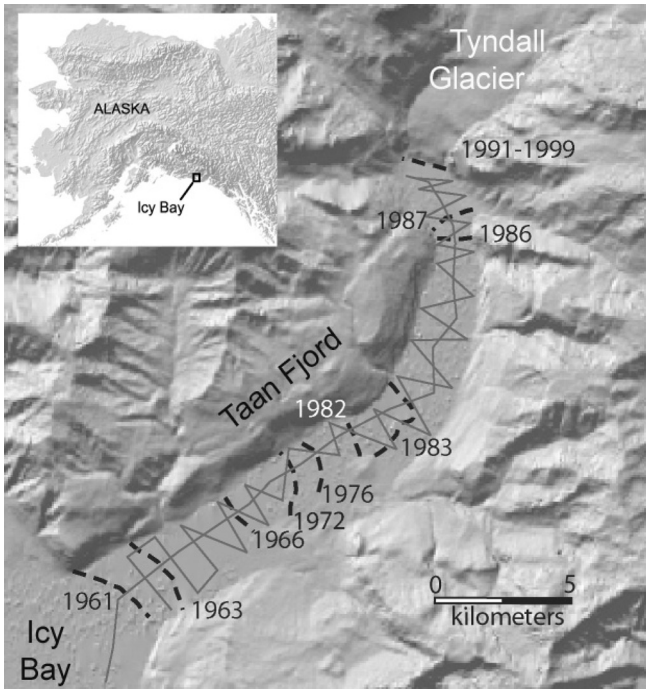

Figure 2. DEM of Taan Fjord showing ice retreat history and track lines from 1999 seismic survey. Track lines are marked by shaded lines; ice margin positions were derived from USGS aerial photos and *Porter* [1989]. Inset shows location of Icy Bay and Taan Fjord within Alaska.

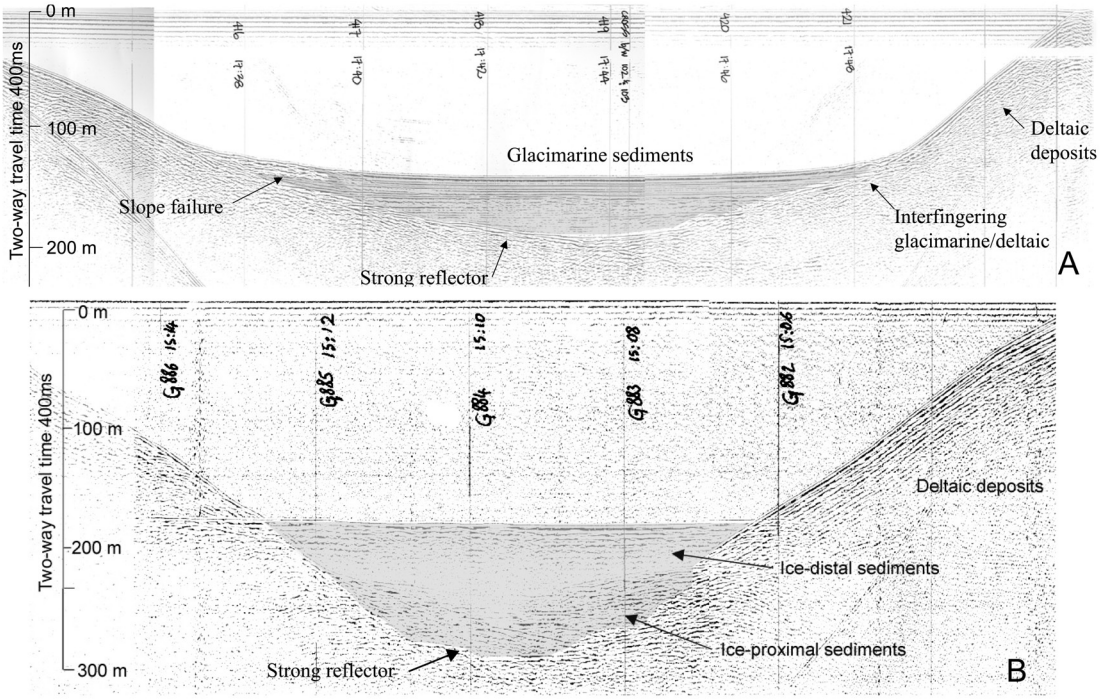

Figure 3. Sample acoustic profiles from which sediment thicknesses measured (a) from lower Taan Fjord (in vicinity of 1966 terminus position) and (b) from upper Taan Fjord (in vicinity of 1989 terminus position). Laminated, semitransparent facies are interpreted as distal glacimarine deposits, while chaotic, hummocky facies represent ice-proximal deposits and laminated, hummocky facies represent fan delta complexes. The strong reflector underlying all three facies is assumed to be indicative of compression and dewatering of the underlying sediments, or Yakataga glacimarine "bedrock," by overriding ice and/or sediment.

sediments overridden by the glacier as it advanced to its Little Ice Age maximum position or retreated back to the mouth of Taan Fjord. We determined sediment thickness from time delays recorded in seismic profiles using seismic velocities of 1460 ms^{-1} for seawater and 1680 ms^{-1} for poorly consolidated glacimarine muds. The latter seismic velocity is known to within 3%, as measured seismic velocities for glacimarine tills and muds range from 1640 ms^{-1} to 1740 ms^{-1} s [*Stoker et al.*, 1997; *Hunter and Pullan*, 1990]; hence we estimate uncertainties in sediment thickness to be of the same order of ~3%. We digitized key horizons in the seismic profiles and extrapolated the upper and lower surfaces bounding the unconsolidated sediments to the fjord edges between the dense track lines of our acoustic profiling survey using a triangular irregular network (TIN) in ArcINFO. The maximum distance between track lines was approximately 500 m. Assuming that sediment reworking through turbidity flows and slumping is efficient at smoothing the sediment surface, as noted by *Jaeger and Nittrouer* [1999], the piecewise planar surface of the reconstructed bed using the TIN method appears to adequately represent the sediment surface between track lines, and represents the bedrock surface with 15% uncertainty (comparison of our TIN grid with seismic profiles revealed a root-mean-square difference of approximately 10 m; because of the general concavity of the bedrock subsurface in the fjord and low relief of the upper sediment surface, the TIN method tends to underestimate the sediment thickness). We identified all obvious delta fan complexes and fjord wall slumps by their seismic facies and excluded them from the sediment thickness measurements.

[12] The sediment thicknesses reconstructed using the TIN method were contoured and the resulting map is shown in Figure 4. Uncertainties arise from our estimates of the seismic velocity of the glacimarine sediments, as mentioned previously, as well as from interpolation of the sediment and bedrock surfaces. All uncertainties, including minor errors in digitizing, as well as the potential for some submarine fan facies to be interfingered with distal glacimarine sediments along the fan edge and thus erroneously included in the volume computation, collectively result in an estimated 20% uncertainty in glacimarine sediment thickness in the fjord.

[13] The total postglacial sediment volume in Taan Fjord as of 1999 was 5.6×10^8 m^3. Assuming the entire sediment package was deposited between 1962 and 1999, the annual flux of sediment into Taan Fjord over the 37-year period has averaged 1.5×10^7 m^3a^{-1}.

3.2. Subaerial Sediment Contribution

[14] The delta fan complexes imaged in the seismic profiles reflect point sources of subaerial sediments derived not from Tyndall Glacier but from tributary streams first highlighted by *Meigs* [1998] and *Meigs et al.* [2002]. Several actively prograding deltas were identified in our seismic survey and can be seen contributing significant

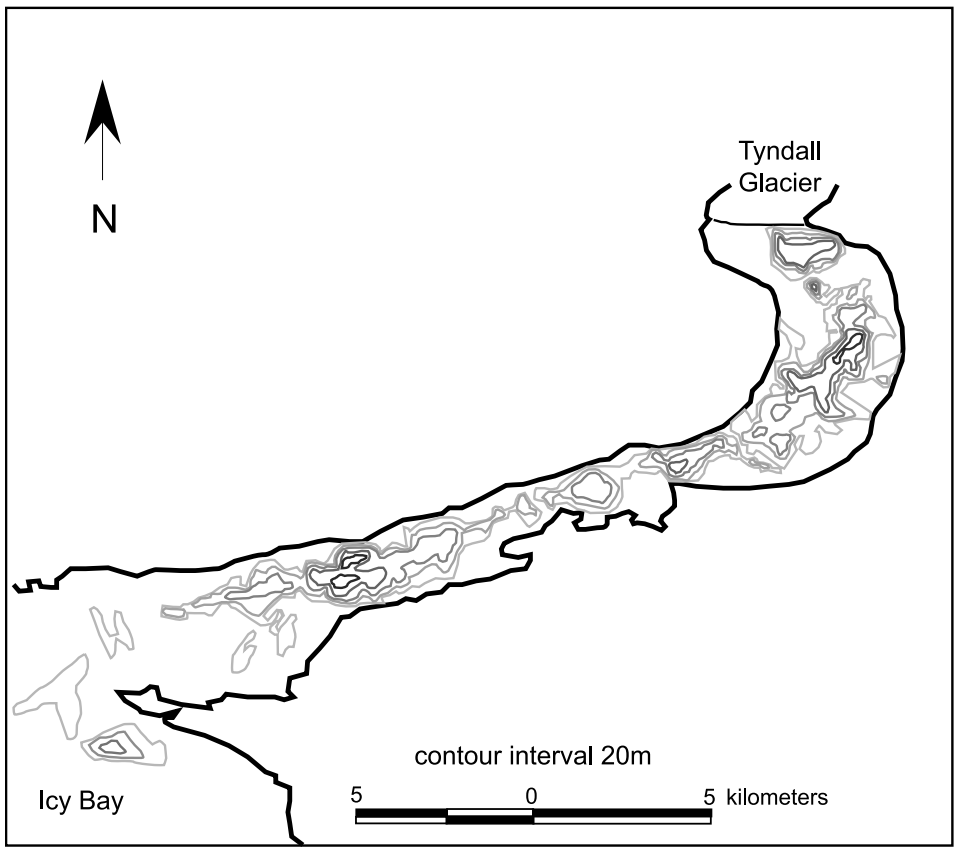

Figure 4. Contours of sediment thickness in Taan Fjord, from 1999 seismic survey of fjord sediments, derived from surface and subsurface reflectors. The lightest contour is 10 m, with a subsequent contour interval of 20 m. The maximum sediment thickness is 90 m. Projection is in Lambert conical.

sediment to the fjord in turbid plumes visible in aerial photos and in a 1996 Landsat 7 image, which begs the questions of what proportions of the delta fan complexes were imaged and excluded from our measurements in the seismic surveys, and how much of the fine sediments from these streams was deposited distally in the fjord and would appear indistinguishable from the distal glacimarine facies. On the basis of their large, recently excavated valleys, as well as their large sediment plumes in the Landsat image, two major streams stand out as obvious contributors to the sediment accumulation in the fjord: the Hoof Hill stream and the 1974 Moraine stream (Figure 5). The lower reaches of both valleys were blocked by Tyndall Glacier throughout much of the past century, as recorded in aerial photos of the glacier system since 1938 (see Figure 1). Aerial photos from 1958 (lower fjord) and 1986 (upper fjord) show sediment backfilling the valleys nearly to the glacier surface, approximately 350 m.a.s.l. in the upper fjord and 270 m.a.s.l. in the lower fjord (elevations were obtained from SRTM DEM data, and accuracy is approximately 50 m). The sediment in these valleys is glaciofluvial in origin, presumed to be deposited both laterally from the main trunk of Tyndall glacier, as well as from streams eroding the ice-free valleys in the Chaix Hills to the east of the fjord. Although there are several other tributary valleys contributing delta fan complexes to Taan fjord, especially on the west side of the fjord, these valleys were filled by tributary glaciers that merged with Tyndall Glacier as recently as 1986. Hence we have counted them as part of the glacial contribution to the fjord sediments rather than nonglacial, fluvial sources, although we note their potential importance in the transfer of a significant pulse of sediment to the fjord as both tributary and trunk glaciers retreated.

[15] To determine the volume of fluvial sediment that was rapidly transferred from both major tributary valleys to the fjord since the glacier retreated we compared the original sediment surfaces in the valleys to the incised valley surface as of February 2000, using a 15 m digital elevation model (DEM) generated from SRTM data. The original surface was identified in aerial photos, and was assumed to extend to the edge of the fjord, which we believe may overestimate the volume of sediment evacuated from the valley by 20% or more. This sediment surface cannot be identified clearly in the photos because it extended partially under and around tongues of ice that intruded laterally from Tyndall glacier. The surface probably did not extend all the way to the fjord edge, but rather sloped steeply toward the fjord. Using the ArcGIS package, the difference between the original and the 2000 surface was calculated and compared to the sediment volume in the associated alluvial fan complex prograding into the modern fjord. The sediment volume in the fans was calculated using the SRTM DEM data for the portion of the fans that have prograded into the fjord above sea level, and the seismic profiles for the submarine portion. The volume of sediment removed from the valleys exceeded the volume in the fans substantially, indicating that a significant fraction

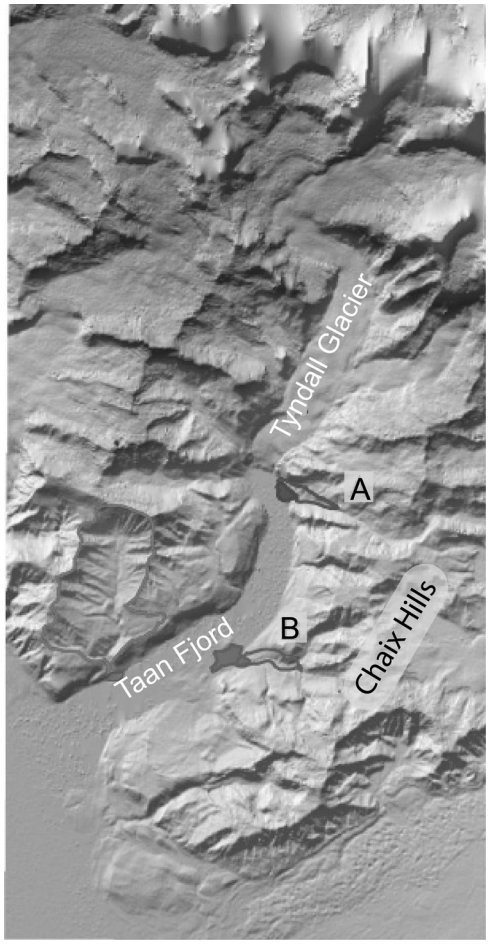

Figure 5. DEM of Taan Fjord and Tyndall Glacier, derived from February 2000 SRTM data. The prograding deltas and back-filled basins of the two predominant nonglacial streams contributing sediment to the fjord are outlined (basin) and filled (delta): A, Hoof hill; B, 1974 Moraine.

of the sediment may have been transported past the fans to the center of the fjord, presumably through remobilization by sediment gravity flows and shallow turbidity plumes [*Jaeger and Nittrouer*, 1999; *Syvitski*, 1989].

[16] In total, we estimate that at most 15.6×10^7 m^3 of sediment was removed from Hoof Hill valley since 1989, of which 4.1×10^7 m^3 and 4.5×10^7 m^3 are now in the delta and submarine fan, respectively. The remaining 7.0×10^7 m^3 was deposited more distally in the fjord bottom, and is indistinguishable from the distal glacimarine facies. This distal subaerial sediment contribution is significant, accounting for 12% of the total postglacial sediment volume in the fjord. Locally it is even more dominant. If we assume that the finer sediment from Hoof Hill valley did not start accumulating in the fjord bottom until the glacier had retreated past the valley in 1988–1989, and that both this subaerial sediment and the sediment delivered by Tyndall glacier since 1990 have been largely confined to the upper 5 km of the fjord (in part because of a strong gyre at the head of the fjord observed in the field and in Landsat imagery), it accounts for up to 80% of the infilling in the uppermost basin of the fjord. The large input of fine sediment from Hoof Hill valley is perhaps in part due to the valley being the surface expression of an active strike-slip fault between the Coal Creek and Kultieth Formations [*Plafker et al.*, 1994]. This highly fractured bedrock and significant fault gouge would be readily eroded and transported by the tributary stream.

[17] A similar calculation for the 1974 Moraine stream suggests that it has contributed 1.71×10^7 m^3 of finer sediment to the fjord beyond the delta, or 3% of the total volume of fjord sediment. Thus these two streams, which we observed to be the two most significant generators of nonglacial fine sediment to the fjord system during the past few decades, account for ~15% of the postglacial sediment in the fjord. This value may slightly underestimate the subaerial contribution, however, as we have not accounted for the potential contribution of other sources of fine sediment such as gullying of the fjord walls. Although we have no quantitative data on this more distributed sediment source, the relative size and number of gullies suggest that their collective contribution is minor. More precise definition of the longer-term relaxation of the postglacial landscape will require direct measurement of this "distributed" subaerial sediment input.

4. The 40-Year Average Sediment Flux and Glacial Erosion Rate

[18] After accounting for the subaerial sediment input into the fjord since retreat, our seismic data show that Tyndall Glacier has produced, on average, 1.3×10^7 m^3 of sediment annually.

[19] To arrive at basin-averaged glacial erosion rates, we divide the sediment flux by the contributing basin area, and take into account the difference in density between the eroded bedrock and the sediment in the fjord. We assume an average bedrock density, ρ_{rock}, of 2700 kg m^{-3}, which is appropriate for the crystalline bedrock underlying Tyndall Glacier. Prior to 1991, the glacier was also overriding the less dense Yakataga glacimarine sediments that underlie the lower basin; hence, if parts of the Yakataga Formation were eroded to contribute to the sediment flux, our use of the average bedrock density underestimates the rate of bedrock erosion in that part of the basin. To assure that our calculations do not overestimate bedrock erosion rates we use the lower end of known glacimarine sediment densities, ρ_{sed}, which range from 1700 kg m^{-3} to 2000 kg m^{-3}. For our calculated average sediment flux of $Q_{sed} = 1.3 \times 10^7$ m^{3}a^{-1}, the average flux of eroded bedrock from Tyndall Glacier ($Q_{rock} = \rho_{sed} Q_{sed} / \rho_{rock}$) divided by the contributing basin area (256 km^2 for the watershed in 1959, decreasing in a stepwise fashion to 154 km^2 by 1991, as measured from SRTM DEM data imported into ArcGIS), yields a basin-averaged erosion rate of 28 ± 5 mma^{-1} for the past 40 years.

5. Temporal Variation in Sediment Flux From Tyndall Glacier

[20] To explore the temporal dimension of sediment production by Tyndall Glacier, we use a simple numerical model of glacimarine sedimentation that enables us to calculate the annual sediment output needed to produce

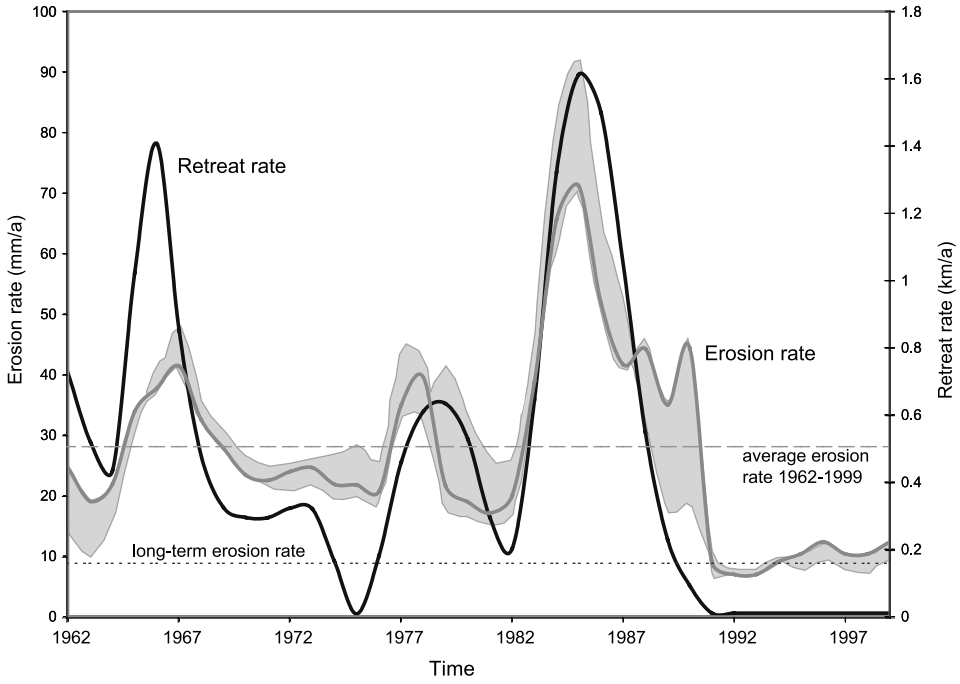

Figure 6. Comparison of erosion rate and retreat rate for Tyndall Glacier since 1962. Average contemporary erosion rate for 1962–1999 is 28 ± 5 mm a^{-1}. Shading indicates the range of erosion rates produced using a range of critical slope angles for sediment reworking in the fjord.

the sediment package observed in the proglacial fjord of any retreating tidewater glacier with a known retreat history (described by *Koppes and Hallet* [2002]). The thickness of sediment at any one point in the fjord reflects a combination of two distinct rates: the variable rate of sediment delivery to the terminus, and the rate of terminus retreat. Where one of these parameters is known, and the total sediment volume in the fjord is measured, the other parameter can be calculated, given the relationship

$$S = \int_0^t \dot{S}(x,t)dt = \int_0^t \dot{S}_0 e^{-\dot{R}t/x*}\,dt \qquad (1)$$

where S is the total sediment thickness, $\dot{S}$ and $\dot{S}_0$ are the time-varying sedimentation rates at a distance x in front of the ice and at the ice front, respectively, $\dot{R}$ is the time-varying rate of terminus retreat and x_* characterizes the distance from the terminus over which the sedimentation rate decreases by 1/e. Our model, which assumes an exponential decrease in sedimentation rate with distance from a tidewater glacier as reported in previous studies [e.g., *Cowan and Powell*, 1991], enables us to reconstruct the temporal variability of the sediment flux as a function of the sedimentation rate at the terminus, S_0(t), for glaciers where the annual retreat rate can be reconstructed from maps and photos, and the total sediment thickness S is known from seismic profiles.

[21] A smoothly varying annual retreat rate of the terminus of Tyndall glacier since 1962 was calculated using a piecewise spline function [*Rasmussen*, 1991] to interpolate between 17 known terminus locations over time. Terminus positions since 1962 were acquired from maps [*Roche*, 1996; *Porter*, 1989], USGS aerial photos and Landsat images. The volume of glacigenic sediment measured in the fjord was parsed into 250 m bins and used as input to our model. By entering the annual retreat rate and the distribution of sediment thickness into the model, we reconstructed the variable annual sediment flux, and hence the erosion rate, from the glacier that is required to account for the observed sediment accumulation (Figure 6). The annual sediment flux necessary to produce the sediment thickness at any point in the fjord is also tempered by the remobilization of sediments in the fjord bottom through sediment gravity flows and turbidity plumes. To model this, at each time step sediment was redistributed between adjacent bins until a critical, effective "angle of repose" was reached [*Jaeger and Nittrouer*, 1999]. We varied this angle of repose for soft sediment under water between 1° to 8°, according to observed submarine slopes in Taan Fjord and similar submarine environments, to calculate the envelope of annual sediment flux, and hence erosion, required from the glacier to produce the fjord sediment package. Decreasing the angle of repose effectively reduced the annual erosion rate required to fill the bins, as the sediment was more evenly distributed in the fjord. The envelope of erosion rates is outlined in grey in Figure 6.

[22] For Tyndall Glacier, the model indicates that the sediment flux, and by inference the erosion rate, generally parallel the retreat rate (Figure 6). During years when the terminus was retreating most rapidly, exceeding 1500 m a^{-1}, basin-wide erosion rates exceeded 90 mm a^{-1}. During years when the ice margin remained stable, such as from 1991–1999, the rate of erosion dropped to 7–9 mm a^{-1}.

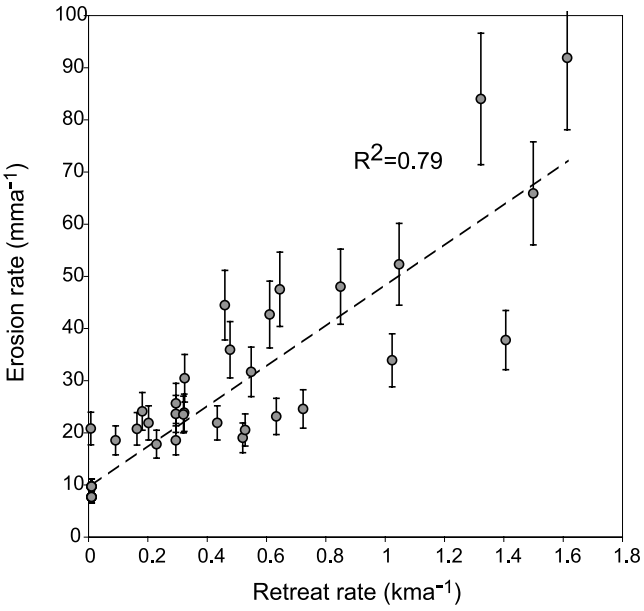

Figure 7. Correlation of erosion rate and retreat rate for Tyndall Glacier since 1962. Error bars indicate a 20% uncertainty in calculating erosion rates. Extrapolating the erosion rate to times when the glacier is effectively stable, the long-term erosion rate is 9 ± 2 mm a^{-1}.

Most notably, the erosion rate and retreat rate are strongly correlated ($R^2 = 0.79$) (Figure 7).

6. Implications for Long-Term Erosion by Alaskan Glaciers

[23] Most tidewater glaciers spend significantly longer periods of their cycle in an advance phase or quasi-stable mode, and tend to retreat quite quickly at the end of the cycle [*Meier and Post*, 1987]. Tyndall Glacier is a perfect example: it first started to advance out of Taan Fjord around 1400 A.D., reached its Little Ice age maximum at the mouth of Icy Bay sometime before 1794 A.D. (when Captain Vancouver first sailed by and mapped the ice extending out of the bay), and began to retreat quite rapidly in 1905, reaching the mouth of Taan fjord in 1961 [*Porter*, 1989]. The rate of advance through lower Icy Bay averaged 60 m a^{-1}, lasting almost 400 years, while the rate of retreat for the period until 1961 averaged 450 m a^{-1}, lasting only 60 years, with over 100 years of standstill in between.

[24] In order to interpret the ''long-term'' erosion rate for Tyndall Glacier on millennial timescales (i.e., over one or several glacial advance-retreat cycles), we assume the correlation between erosion rate and retreat rate can be extrapolated to periods of no retreat, represented by the intercept of a linear best fit relationship of the data. The extrapolated erosion rate is the best estimate we have of the rate of erosion during periods of standstills, such as at the peak of the Little Ice Age. During the protracted advance phase the rate of bedrock erosion may tend to be less than during standstills because, at least in the lower reaches of the glacier, considerable proglacial sediment has to be evacuated before the glacier can erode the bed. Accordingly, since a substantial portion of a normal tidewater glacier cycle is spent in a quasi-stable phase, and the relatively short period of rapid erosion during the retreat phase tends to be offset by the slower bedrock erosion during the longer advance phase, we assume that the extrapolated erosion rate for periods of standstill, represented by the y-intercept in Figure 7, is most representative of the ''long-term'' erosion rate for Tyndall Glacier. This long-term erosion rate is 9 ± 2 mm a^{-1}. It is 3.5 ± 1.5 times lower than the recent 40-year average rate, and an order of magnitude lower than the peak erosion rate circa 1985, when Tyndall was retreating most rapidly.

[25] Our results showing that sediment yields are high when Tyndall Glacier retreats rapidly, together with similar results for Muir Glacier [*Koppes and Hallet*, 2002], suggest that most of the sediment yield data from tidewater glaciers in Alaska collected to date correspond to contemporary erosion rates that are significantly higher than those in the long term. We have confidence that this bias toward unusually high sediment yields in the short term is applicable to other published rates of erosion for Alaskan tidewater glaciers, since all the other studies [e.g., *Molnia et al.*, 1984; *Powell*, 1991; *Cowan and Powell*, 1991; *Hunter et al.*, 1996; *Jaeger and Nittrouer*, 1999] were measured using similar methods from calving glaciers that have also been in steady retreat since the end of the Little Ice Age (with the exception of Taku Glacier [*Motyka et al.*, 2005]). At Muir Glacier, we found that contemporary rates of erosion were a factor of five higher than the long-term rate. Accordingly, we present a revision of the compilation of glacial erosion rates originally published by *Hallet et al.* [1996] in which contemporary rates for all Alaskan basins drained by tidewater glaciers are reduced by a factor of four to conservatively approach their ''long-term'' rates, such as those we derived for both Tyndall Glacier and Muir Glacier (Figure 8).

7. Implications for Controls on Glacier Erosion

[26] The strong correlation we found between erosion rate and retreat rate for Tyndall Glacier (and for Muir Glacier) is not surprising if we presume both that ice velocity is proportional to retreat rate, as was observed for another tidewater glacier in the region, Columbia Glacier [*Van der Veen*, 1996], and that sediment delivery to the terminus increases with glacial sliding speed, as was documented for Variegated Glacier [*Humphrey and Raymond*, 1994] and Bench Glacier [*Riihimaki et al.*, 2005].

[27] In the case of Columbia Glacier, the inception of terminus retreat in 1982 was accompanied by a concomitant increase in glacier surface speed, which was associated with thinning near the terminus and assumed to be due to an increase in surface slope and along-flow stretching as ice was drawn down through the glacier system [*Van der Veen*, 2002; *Brown et al.*, 1982]. Unfortunately, we do not have any measurements of glacier speed for Tyndall Glacier throughout our study period to make a similar comparison. Two observations, however, support the suggestion that during this period of retreat the speed of Tyndall glacier was higher than average. First, the surface slope increased along the length of the glacier from 3.9° in 1961 to 6.5° in 1999, as the total glacier length decreased by half. Second, the ice flux into Taan fjord necessary to reduce the glacier

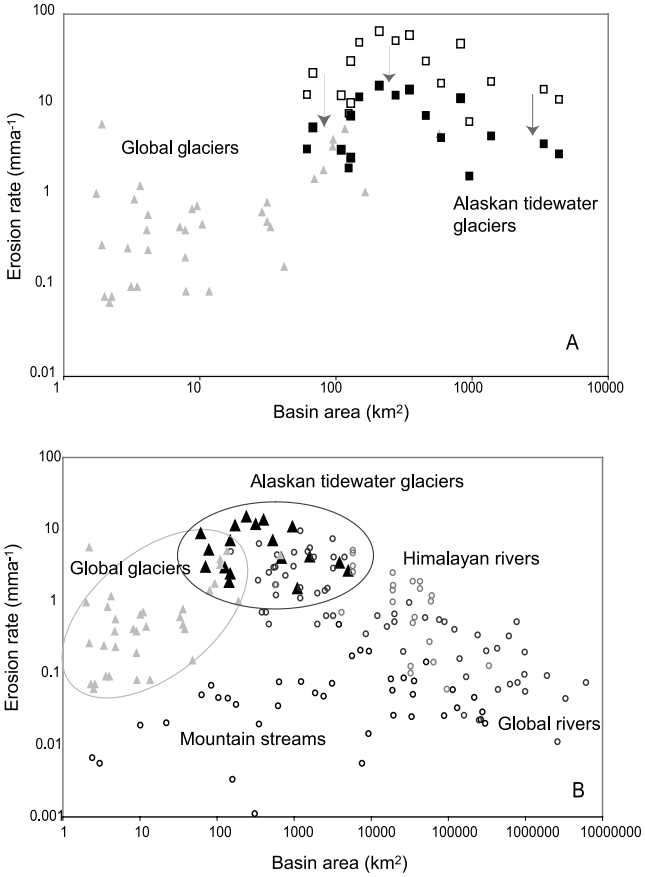

Figure 8. Erosion rates for glacial and nonglacial basins, revised from data originally compiled by *Hallet et al.* [1996] by reducing contemporary rates derived from retreating tidewater glaciers in SE Alaska (open squares) by a factor of 4 to estimate long-term erosion rates (solid squares). This reduction is based on our estimate that tidewater glaciers undergoing rapid retreat produce sediment ~4 times faster than in the long term (see text). (a) Erosion rates for glacial basins, including tidewater glaciers in SE Alaska (solid squares) and glacial erosion rates (shaded triangles) elsewhere in the world. (b) Comparison of glacial erosion rates (triangles) and fluvial erosion rates (circles) from global rivers [*Milliman and Syvitski*, 1992], mountain basins in British Columbia [*Church and Slaymaker*, 1989] and mountain basins in the high Himalaya.

volume and draw down its surface must have exceeded the balance flux considerably, since most of the ice in these tidewater glacier systems is lost by calving. In just 40 years of retreat, approximately half of the total volume of the glacier in 1961 has been lost ($\sim 3.19 \times 10^{10}$ m^3), and the glacier thickness has decreased over ~300 m at the present glacier terminus and in decreasing amounts toward the drainage divide. These decreases in ice thickness along the glacier are of the same magnitude as the accumulation of ice expected over the glacier over the 40-year period, using a plausible accumulation rate of 2–3 m a^{-1} [*Wilson and Overland*, 1987]. This suggests that ice fluxes, and by inference basal velocities, may have been roughly twice their long-term (i.e., balance) values during this time.

[28] Increases in ice velocity can increase glaciofluvial sediment flux to the terminus either through accelerated erosion of bedrock, or through enhanced evacuation of sediments stored under the glacier. Englacial and supraglacial sediment flux will also increase with increasing ice flux to the terminus, but these sources of sediment are of an order of magnitude smaller than the glaciofluvial sediment flux [e.g., *Hunter et al.*, 1996], and hence would not significantly affect the overall sediment output of the glacier. Decreases in subglacial sediment storage may be significant in the short term such as during a surge, periods of local ice acceleration and subglacial cavity expansion [e.g., *Anderson et al.*, 2004], or at the start of the melt season when efficient subglacial water conduits start to form. At Variegated Glacier, both the sediment yield at its outlet streams and sliding speed increased by two orders of magnitude during a surge in 1981–1982 [*Humphrey and Raymond*, 1994]. At Bench Glacier, periods of enhanced sliding at the start of the melt season during three consecutive years were accompanied by increases in both sediment and water discharge [*Riihimaki et al.*, 2005]. In both of these examples, the pulse of sediment discharge could be related not only to increased glacier sliding but also to short-term changes in efficiency of the subglacial hydrologic system. A sudden increase in the water discharge would evacuate sediments more readily and enhance the correlation between glacier sliding and sediment flux for short periods.

[29] Such increases in water discharge, however, could not be sustained over decades to account for the massive sediment flux from Tyndall Glacier. Likely volumes of sediment stored beneath Tyndall Glacier are but a small fraction of the sediment delivered to Taan Fjord during the 40-year period examined in this study. To attribute this increase in sediment flux solely to enhanced evacuation of stored sediments under Tyndall Glacier would require the removal of a ~20 m-thick layer of basal sediment stored under the entire ablation area of the glacier (~25 km^2), where such debris is most likely to accumulate. Such a requisite thickness of mobile basal debris is excessive compared to the characteristic thickness of only a few decimeters that has been documented in the few boreholes that have penetrated to the base of coastal Alaskan glaciers, such as Columbia Glacier [*Humphrey et al.*, 1993] and Variegated Glacier [*Kamb et al.*, 1985]. Only in one instance has up to 7 m of mobile debris been cored and instrumented, under Black Rapids Glacier [*Truffer et al.*, 1999]; in this case, evacuation of basal debris *could* cause periodic increases in sediment flux. Such rapid debris evacuation could only be sustained, however, if it was offset by rapid erosion. Moreover, a thick blanket of basal debris would preclude bedrock erosion as it would tend to prevent sliding ice from having direct access to the underlying bedrock.

[30] Recent studies of the evacuation of proglacial and subglacial debris by Taku Glacier during its current advance document the evacuation of approximately 1.9 m a^{-1} of soft sediment during the 20th century, flushed from beneath the advancing snout [*Motyka et al.*, 2005]. Such rapid evacuation of unconsolidated sediment, approaching 200 m per century, provides confidence in our assumption that all the sediment stored subglacially, as well as in the fjord, prior to

the last advance of Tyndall Glacier had been effectively removed and transferred to the Gulf of Alaska long before the retreat of the ice from Taan Fjord nearly five centuries later. Hence the large sediment flux we have documented at Tyndall Glacier most probably reflects enhanced bedrock erosion due to accelerated basal ice motion associated with rapid retreat, with only a minor contribution derived from the relatively small volume of sediment likely to be stored subglacially.

[31] The long-term erosion rate of 9 ± 2 mm a^{-1} that we derive for Tyndall glacier approaches the maximum expected tectonic uplift rates [e.g., *Bird*, 1996] in the region. Our proposed extrapolation of contemporary sediment yields to obtain long-term erosion rates therefore helps resolve the apparent conundrum of contemporary erosion rates exceeding tectonic uplift rates significantly: In the long term, the two must balance each other to maintain the relief that is known to have existed in the region over millions of years. It remains of interest, however, that our derived long-term erosion rates are still significantly higher than those inferred from the simplest possible interpretations of the thermochronology of the region [*Spotila et al.*, 2004]. We suggest two possible reasons for this discrepancy. One is that the erosion rates inferred from thermochronology, which represent temporal averages over periods of order 10^6 years, are actually lower than those for shorter periods of order 10^3 years with which we are concerned. Alternatively, some of the poorly constrained assumptions required for the interpretations of the thermochronology may lead to unreliable estimates of exhumation rates. Notably, the simple, common assumption that packets of crustal material follow vertical trajectories to the surface, whereas ascent along paths that are in general gently inclined is more likely in this tectonic setting, would tend to underestimate cooling rates and, hence, exhumation rates substantially.

8. Conclusions

[32] Our model of proglacial sedimentation reveals a clear correlation between glacial retreat rates and glacial sediment yields from Tyndall glacier, which we believe reflects the tendency for ice velocities to increase with retreat rates and for glacial erosion rates to scale with ice velocity. Taking into account the correlation between sediment flux and retreat rate, and the remobilization of subaerial sediments formerly ponded by ice, the long-term erosion rate for Tyndall Glacier is 9 ± 2 mm a^{-1}. The significant contribution of subaerial sediments to the fjord system, which composed $\sim$15% of the total volume of postglacial sediments in Taan Fjord, is a product of the immediate response of the landscape to changing base levels following glacial retreat.

[33] Our results showing that sediment yields are high when Tyndall glacier retreats rapidly, together with similar results for Muir Glacier [*Koppes and Hallet*, 2002], imply that most sediment yield data from tidewater glaciers in Alaska over the last century correspond to contemporary erosion rates that are a factor of 3.5 ± 1.5 higher than in the long term. Contemporary glacier erosion rates in Alaska and elsewhere are high because rapid retreat has been characteristic of the entire period of study, extending back to the end of Little Ice Age. For many of these heavily glaciated basins, even the improved estimates of long-term erosion rates in southern coastal Alaska remain among the highest known rates worldwide, and exceed million year timescale exhumation rates derived from low-temperature thermochronometry in the region.

[34] **Acknowledgments.** We thank Austin Post for providing us access to a wealth of unpublished data, Dick Sylwester for leading the seismic surveys, Yann Merrand and Alison Anders for help in the field, Gretchen Moore for many hours spent manipulating analog data sets into ArcINFO format and drafting maps, Al Rasmussen for helping us interpolate terminus retreat data, and Andrew Meigs for stimulating discussion regarding the genesis of the sediments in Taan Fjord. We also thank Roger LeB. Hooke, Neal Iverson and an anonymous reviewer for many helpful comments on the draft manuscript. This work was funded by National Science Foundation grant EAR-9628675 and a University of Washington fellowship to Koppes.

References

Anderson, R. S., S. P. Anderson, K. R. MacGregor, E. D. Waddington, S. O'Neel, C. A. Riihimaki, and M. G. Loso (2004), Strong feedbacks between hydrology and sliding of a small alpine glacier, *J. Geophys. Res.*, *109*, F03005, doi:10.1029/2004JF000120.

Beaumont, C., J. A. Munoz, J. Hamilton, and P. Fullsack (2000), Factors controlling the Alpine evolution of the central Pyrenees inferred from a comparison of observations and geodynamical models, *J. Geophys. Res.*, *105*, 8121–8145.

Bird, P. (1996), Computer simulations of Alaskan neotectonics, *Tectonics*, *15*, 225–236.

Brown, C. S., M. F. Meier, and A. Post (1982), Calving speed of Alaska tidewater glaciers, with application to Columbia Glacier, *U.S. Geol. Surv. Prof. Pap. 1258-C*, 13 pp.

Brozovic, N., D. W. Burbank, and A. J. Meigs (1997), Climatic limits on landscape development in the northwestern Himalaya, *Science*, *276*, 571–574.

Bruhn, R. L., T. L. Pavlis, G. Plafker, and L. Serpa (2004), Deformation during terrane accretion in the Saint Elias Orogen, Alaska, *Geol. Soc. Am. Bull.*, *116*, 771–787.

Church, M., and O. Slaymaker (1989), Disequilibrium of Holocene sediment yield in glaciated British Columbia, *Nature*, *337*, 452–454.

Cowan, E. A., and R. Powell (1991), Ice-proximal sediment accumulation rates in a temperate glacial fjord, southeastern Alaska, in *Glacial Marine Sedimentation: Paleoclimatic Significance*, edited by J. B. Anderson and G. M. Ashley, *Geol. Soc. Am. Spec. Pap.*, *261*, 61–74.

Elverhøi, A., R. L. Hooke, and A. Solheim (1998), Late Cenozoic erosion and sediment yield from the Svalbard-Barents Sea region: Implications for understanding erosion of glacierized basins, *Quat. Sci. Rev.*, *17*, 209–241.

Finlayson, D., D. R. Montgomery, and B. Hallet (2002), Spatial coincidence of rapid inferred erosion with young metamorphic massifs in the Himalayas, *Geology*, *30*, 219–222.

Gurnell, A., D. Hannah, and D. Lawler (1996), Suspended sediment yields from glacier basins, in *Erosion and Sediment Yield: Global and Regional Perspectives*, edited by D. E. Walling, and B. W. Webb, *IAHS Publ.*, *236*, 97–104.

Hallet, B., L. Hunter, and J. Bogen (1996), Rates of erosion and sediment evacuation by glaciers: A review of field data and their implications, *Global Planet. Change*, *12*, 213–235.

Humphrey, N. F., and C. F. Raymond (1994), Hydrology, erosion and sediment production in a surging glacier: Variegated Glacier, Alaska, 1982–1983, *J. Glaciol.*, *40*, 539–552.

Humphrey, N. F., B. Kamb, M. Fahnestock, and H. Engelhardt (1993), Characteristics of the bed of the lower Columbia Glacier, Alaska, *J. Geophys. Res.*, *98*, 837–846.

Hunter, J. A., and S. E. Pullan (1990), A vertical array method for shallow seismic refraction surveying of the sea floor, *Geophysics*, *55*, 92–96.

Hunter, L. E., R. D. Powell, and D. E. Lawson (1996), Flux of debris transported by ice at three Alaskan tidewater glaciers, *J. Glaciol.*, *42*, 123–135.

Jaeger, J. M., and C. A. Nittrouer (1999), Sediment deposition in an Alaskan fjord: Controls on the formation and preservation of sedimentary structures in Icy Bay, *J. Sediment. Res.*, *69*, 1011–1026.

Kamb, B., C. F. Raymond, W. D. Harrison, H. Engelhardt, K. A. Echelmeyer, N. Humphrey, M. M. Brugman, and T. Pfeffer (1985), Glacier surge mechanism: 1982–1983 surge of Variegated Glacier, Alaska, *Science*, *227*(4686), 469–479.

Koppes, M. N., and B. Hallet (2002), Influence of rapid glacial retreat on the rate of erosion by tidewater glaciers, *Geology*, *30*, 47–50.

Lagoe, M. B., C. H. Eyles, N. Eyles, and C. Hale (1993), Timing of late Cenozoic tidewater glaciation in the far North Pacific, *Geol. Soc. Am. Bull.*, *105*, 1542–1560.

Meier, M. F., and A. Post (1987), Fast tidewater glaciers, *J. Geophys. Res.*, *92*, 9051–9058.

Meigs, A. (1998), Bedrock landsliding accompanying deglaciation: Three possible examples from the Chugach/St. Elias Range, Alaska, *Eos Trans. American Geophysical Union*, *79*(45), Fall Meet. Suppl.

Meigs, A., W. C. Krugh, K. Davis, and G. Bank (2002), Ultra-rapid landscape response and sediment yield following glacier retreat, Icy Bay, southern Alaska, *Eos Trans. AGU*, *83*(44), Fall Meet. Suppl., Abstract T12E-08.

Milliman, J. D., and J. P. M. Syvitski (1992), Geomorphic/tectonic control of sediment discharge to the ocean: The importance of small mountainous rivers, *J. Geol.*, *100*, 525–544.

Molnar, P., and P. England (1990), Late Cenozoic uplift of mountain ranges and global climate change: Chicken or egg?, *Nature*, *346*, 29–34.

Molnia, B. F. (1979), Sedimentation in coastal embayments in the northern Gulf of Alaska, paper presented at Offshore Technology Conference, Houston, Tex.

Molnia, B. F., T. J. Atwood, P. R. Carlson, A. Post, and S. C. Vath (1984), Map of marine geology of upper Muir and Wachusett Inlets, Glacier Bay, Alaska: Sediment distribution and thickness, bathymetry and interpreted seismic profiles, *U.S. Geol. Surv. Open File Map 84-632*.

Montgomery, D. R., G. Balco, and S. D. Willett (2001), Climate, tectonics and the mego-morphology of the Andes, *Geology*, *29*, 579–582.

Motyka, R., E. Kuriger, and M. Truffer (2005), Excavation of sediments by tidewater glacier advance and implications for the oceanic sediment record, Taku Glacier, Alaska, USA, *EGU Geophys. Res. Abstr.*, *7*, 02901.

Plafker, G., J. C. Moore, and G. R. Winkler (1994), Geology of the southern Alaska margin, in *The Geology of Alaska, Geology of North America, G-1*, edited by G. Plafker and H. C. Berg, pp. 389–449, Geol. Soc. of Am., Boulder, Colo.

Porter, S. C. (1989), Late Holocene fluctuations of the fiord glacier system in Icy Bay, Alaska, U.S.A., *Arct. Alp. Res.*, *21*, 364–379.

Post, A. (1983), Preliminary bathymetry of upper Icy Bay, Alaska, *U.S. Geol. Surv. Open File Rep. 83-256*, 1 sheet.

Powell, R. D. (1991), Grounding-line systems as second-order controls on fluctuations of tidewater termini of temperate glaciers, in *Glacial Marine Sedimentation: Paleoclimatic Significance*, edited by J. B. Anderson and G. M. Ashley, *Geol. Soc. Am. Spec. Pap.*, *261*, 75–94.

Rasmussen, L. A. (1991), Piecewise integral splines of low degree, *Comput. Geosci.*, *17*, 1255–1263.

Raymo, M. E., and W. F. Ruddiman (1992), Tectonic forcing of late Cenozoic climate, *Nature*, *359*, 117–122.

Riihimaki, C. A., K. R. MacGregor, R. S. Anderson, S. P. Anderson, and M. G. Loso (2005), Sediment evacuation and glacial erosion rates at a small alpine glacier, *J. Geophys. Res.*, *110*, F03003, doi:10.1029/2004JF000189.

Roche, J. W. (1996), Lithologic controls on rapid frost-induced breakdown of rock, Icy Bay, Alaska: Implications for enhanced sediment production during glacial-interglacial cycles, M.S. thesis, Univ. of Wash., Seattle.

Spotila, J., J. Buscher, A. Meigs, and P. Reiners (2004), Long-term glacial erosion of active mountain belts: Example of Chugach-St. Elias range, Alaska, *Geology*, *32*, 501–504.

Stoker, M. S., J. B. Pheasant, and H. Josenhans (1997), Seismic methods and interpretation, in *Glaciated Continental Margins: An Atlas of Acoustic Images*, edited by T. A. Davies et al., pp. 9–26, CRC Press, Boca Raton, Fla.

Syvitski, J. P. M. (1989), On the deposition of sediment within glacier-influenced fjords: Oceanographic controls, *Mar. Geol.*, *85*, 301–329.

Tomkin, J. H. (2003), Erosional feedbacks and the oscillation of ice masses, *J. Geophys. Res.*, *108*(B10), 2488, doi:10.1029/2002JB002087.

Truffer, M., R. J. Motyka, W. D. Harrison, K. A. Echelmeyer, B. Fisk, and S. Tulaczyk (1999), Subglacial drilling at Black Rapids Glacier, Alaska, USA: Drilling methods and sampling results, *J. Glaciol.*, *45*(151), 495–505.

Van der Veen, C. J. (1996), Tidewater calving, *J. Glaciol.*, *42*, 375–385.

Van der Veen, C. J. (2002), Calving glaciers, *Prog. Phys. Geogr.*, *26*(1), 96–122.

Wilson, J. G., and J. E. Overland (1987), Meteorology, in *The Gulf of Alaska: Physical Environment and Biological Resources*, edited by D. W. Hood and S. T. Zimmerman, pp. 31–56, NOAA, U.S. Dep. of Commer., Washington, D. C.

Zeitler, P. K., et al. (2001), Erosion, Himalayan geodynamics and the geology of metamorphism, *GSA Today*, *11*, 4–8.

B. Hallet and M. Koppes, Department of Earth and Space Sciences, University of Washington, Seattle, WA 98195, USA. (koppes@u.washington.edu)